HHS Public Access

Author manuscript

Sci Transl Med. Author manuscript; available in PMC 2015 March 11.

Published in final edited form as:

Sci Transl Med. 2014 July 30; 6(247): 247ra103. doi:10.1126/scitranslmed.3008490.

Asc-1, PAT2 and P2RX5 are novel cell surface markers for white, beige and brown adipocytes

Siegfried Ussar[1,2], **Kevin Y. Lee**[1], **Simon N. Dankel**[1,3,4], **Jeremie Boucher**[1], **Max-Felix Haering**[1], **Andre Kleinridders**[1], **Thomas Thomou**[1], **Ruidan Xue**[1], **Yazmin Macotela**[1,†], **Aaron M. Cypess**[1], **Yu-Hua Tseng**[1], **Gunnar Mellgren**[3,4], and **C. Ronald Kahn**[1,*]

[1]Section on Integrative Physiology and Metabolism, Joslin Diabetes Center and Harvard Medical School, 02215 Boston, MA, USA

[2]Institute for Diabetes and Obesity, Helmholtz Center Munich, 85764 Neuherberg, Germany

[3]Department of Clinical Science, University of Bergen, 5020 Bergen, Norway

[4]Hormone Laboratory, Haukeland University Hospital, 5020 Bergen, Norway

Abstract

White, beige and brown adipocytes are developmentally and functionally distinct but often occur mixed together within individual depots. To target white, beige and brown adipocytes for diagnostic or therapeutic purposes, a better understanding of the cell surface properties of these cell types is essential. Using a combination of *in silico*, *in vitro* and *in vivo* methods, we have identified three new cell surface markers of adipose cell types. The amino acid transporter Asc-1 is a white adipocyte-specific cell surface protein, with little or no expression in brown adipocytes, whereas the amino acid transporter PAT2 and the purinergic receptor P2RX5 are cell surface markers expressed in classical brown and beige adipocytes in mice. These markers also selectively mark brown/beige and white adipocytes in human tissue. Thus, Asc-1, PAT2 and P2RX5 are membrane surface proteins that may serve as tools to identify and target white and brown/beige adipocytes for therapeutic purposes.

Introduction

Obesity and its co-morbidities are a rapidly growing burden to our health and healthcare system. Fundamental to the development of obesity is an imbalance between caloric intake and energy expenditure, which results in excessive accumulation of lipids within the various white adipose tissue depots. This is, in part, countered by brown adipose tissue (BAT) that

*To whom correspondence should be addressed: c.ronald.kahn@joslin.harvard.edu.
†Current address: Instituto de Neurobiología, Universidad Nacional Autónoma de México (UNAM), Campus UNAM-Juriquilla, 76230 Querétaro, México.

Competing interests: SU and CRK filed a patent application targeting WAT and BAT using the markers described here. The authors declare no other conflicts of interest.

Data and materials availability: All data and materials are publically available.

Author contributions: SU designed and performed experiments and wrote the paper. KYL, SND, JB, MFH, AK, TT, RX, YM, performed experiments. AMC, YHT and GM provided reagents and expert advice. CRK helped design experiments, reviewed data, provided funding and wrote the paper.

can burn excessive calories via uncoupled respiration using mitochondrial uncoupling protein-1 (UCP-1) (1,2).

In addition to classical brown adipose tissue occurring in selected depots of mammals, brown adipocytes can develop within white adipose tissue and intramuscular fat upon chronic cold or β3 adrenergic receptor stimulation (3). These cells have been referred to as beige or BRITE fat, and originate from precursor populations distinct from classical brown fat (4,5,6,7,8). These beige fat cells also exhibit different gene expression patterns from both brown and white adipocytes (7,9,10). These cells, as well as perhaps other unidentified subpopulations of white adipocytes, contribute to the heterogeneity of white fat depots and potentially to the different metabolic risk associated with accumulation of visceral versus subcutaneous fat (11).

Defining adipose depot composition with regard to white, brown and beige adipocyte cell lineages is especially difficult in humans, where brown/beige fat is located in deeper cervical, supraclavicular and paraspinal areas (12,13,14), and consists of a mixture of brown and white adipocytes. Recent studies suggest that brown adipocytes within these human brown fat depots may be a mixture of classical brown and beige adipocytes depending on the exact location of the depot and the depth within the cervical region (7, 15, 16).

As noted above, white, brown and beige adipocytes differ greatly in their function. An increase in white adipose tissue, especially visceral fat, underlies the development of insulin resistance and the metabolic syndrome. In contrast, increasing the amount or activity of brown/beige fat may help improve caloric balance and metabolism and is currently a pathway under investigation for the treatment of obesity and its complications. However, since most adipose-related proteins are common to white and brown adipocytes, many of the currently used drugs intended to modulate white adipose tissue function can also affect BAT and conversely. Thus, novel strategies to selectively target white and brown/beige adipose tissue are needed to find the best balance for avoiding obesity and ameliorate its adverse consequences.

A number of marker genes have been identified to distinguish brown, beige and white adipocyte cell types (7,10,17). These include leptin, Hoxc8 and Hoxc9 for white fat; Tbx1 and Tmem26 for beige fat; and UCP-1, Cidea and Prdm16 for brown fat. These genes have been useful for the characterization of specific isolated adipocyte subtypes, but their usefulness in identifying and targeting distinct adipocyte types in intact tissue or *in vivo* is limited (9,15), as most of these markers represent intracellular or secreted proteins. Furthermore some of these markers, such as Prdm16, are also expressed in non-fat tissues (18). Thus, good surface markers would be very helpful in identifying and targeting different adipocyte sub-populations *in vivo*. In the present study, we have identified specific cell surface markers for white, brown and beige adipocytes using a combination of *in silico*, *in vitro* and *in vivo* approaches. These markers provide novel tools to identify different adipocyte populations in both humans and rodents and potentially target them for therapy *in vivo*.

Results

In silico identification of white adipocyte surface markers

Adiponectin is the most abundant and most specific adipocyte protein (18). However, it is primarily a secreted protein (or adipokine), making it of limited value for identification of intact adipocytes *in vivo*. To identify adipocyte-specific or enriched cell surface proteins, we used the expression pattern of mouse *adiponectin* as a model and searched the Symatlas database (www.biogps.org) that contains data from multiple Affymetrix microarray experiments for genes whose expression correlated with that of *adiponectin* with a coefficient greater than 0.95 (fig. S1, A and B). This list was then filtered for genes with high expression in fat (at least 3 times the mean of all other tissues) that also had lower than mean levels of expression in skeletal muscle, heart, lung, pancreas, cerebellum and cerebral cortex. This yielded three transmembrane proteins: N-acetyltransferase 8-like (Nat8L), prolactin receptor (PRLR) and neuregulin-4 (Nrg4). Of these three, Nrg4 showed the highest mouse adipose tissue specificity (fig. S2 and www.biogps.org) with a correlation coefficient to *adiponectin* of >0.95.

To increase the number of adipocyte-specific surface proteins, we repeated the search for genes whose expression also correlated with *Nrg4*. This identified six candidate genes in addition to *Nrg4* as "adipocyte-specific" membrane proteins: transmembrane protein 120B (Tmem120B, adrenergic β3 receptor (Adrb3), aquaporin-7 (Aqp7), G protein-coupled receptor 81 (Gpr81), fatty acid transporter (SLC27a1/FATP1), and solute carrier family 7 member 10 (SLC7a10/Asc-1 neutral amino acid transporter, y+ system) (fig. S2 and www.biogps.org).

Asc-1 is a white adipocyte surface marker in mice

To confirm the Affymetrix mouse protein expression data, we generated a cDNA tissue library containing 18 tissues from 7-week-old C57Bl/6 male mice, as well as uterus and ovary from female mice, and used this to screen all candidate genes. Mice were perfused with PBS prior to sacrifice to minimize contamination of the tissues with blood cells. Although all tested genes showed a significantly higher expression in adipose tissue compared to other tissues, *Nrg4*, *Aqp7* and *Asc-1* showed the greatest adipose tissue specificity (fig. S2).

Adipose tissue is composed of adipocytes, as well as cells in the stromal vascular fraction (SVF), including blood cells, immune cells, endothelial cells and preadipocytes. To test for the adipocyte specificity of the selected candidate genes, we isolated RNA from purified mouse adipocytes and the SVF from several fat depots. SVF had higher or similar expression of *Gpr81*, *Adrb3*, and *Aqp7* when compared to isolated adipocytes from all adipose tissue depots (fig. S3), whereas expression of *Nrg4*, *Fatp1*, *Tmem120b* and *Asc-1* (fig. S3 and Fig. 1A) were specific to adipocytes. *Asc-1* expression was significantly higher in white adipocytes than in brown adipocytes or any of the SVF fractions (Fig. 1A). In addition *Asc-1* showed ~5 fold higher expression in adipocytes from white fat depots than from brown adipocytes (Fig. 1A). By comparison, there was no difference in *Nrg4*, *FATP1* and *Tmem120b* expression between white and brown adipocytes (fig. S3).

The unique expression pattern for *Asc-1* was confirmed in a second panel of 45 mouse tissues isolated from 7 week-old C57Bl/6 mice perfused with PBS, which revealed the highest expression of *Asc-1* in perigonadal and perirenal white fat, followed by subcutaneous and mesenteric fat (Fig. 1B). Mesenteric fat showed similar expression levels as various regions of the brain a tissue that has been reported to highly express *Asc-1* (19,20) and the expression in the other WAT depots was even higher. Low expression of *Asc-1* was observed in interscapular brown fat, adrenal gland, pancreas and lung (Fig. 1B). The difference in *Asc-1* expression between individual white fat depots and brown fat ranged from 4-fold (mesenteric fat to interscapular brown fat) to 79-fold (perigonadal fat to subscapular brown fat) (Fig. 1B).

Expression of *Asc-1* was unaltered in white adipose tissue of the obese, leptin receptor-deficient *db*/*db* mice compared to lean *db*/+ control mice (Fig. 1C), but increased in BAT of obese *db/db* mice, as well as in subcutaneous white adipose tissue of obese leptin deficient *ob/ob* mice compared to *ob*/+ mice (Fig 1D). Wild type mice fed a high fat diet (HFD) containing 60% calories of fat for 8 weeks also significantly increased expression of *Asc-1* in BAT compared to chow diet (CD) fed animals. (Fig. 1E). The increases in *Asc-1* in BAT are consistent with the accumulation of white adipocytes in brown adipose tissue in obese mice.

Like the freshly isolated stromal vascular fraction, FACS-sorted primary murine preadipocytes from subcutaneous and perigonadal fat (21) expressed very low levels of *Asc-1* compared to mature, *in vitro* differentiated adipocytes derived from these cells (Fig. 1F). In contrast, we were unable to detect *Asc-1* expression in either cultured and differentiated primary brown preadipocytes or white adipocytes, further indicating that *Asc-1* is a marker of mature white adipocytes. This white adipocyte specificity was lost after immortalization of SVF, such that brown adipocytes derived from the SVF of BAT using SV-40 large T antigen began to express this white adipocyte marker (fig. S4).

Western blots of whole tissue lysates from mouse subcutaneous and perigonadal white fat, as well as brown fat, confirmed the expression of *Asc-1* in white, but not brown, fat (Fig. 1G). Immunofluorescent staining for *Asc-1* in differentiated, immortalized murine subcutaneous white adipocytes revealed the expected cell surface staining of *Asc-1* (Fig. 1H), which was further confirmed by Western blotting after membrane fractionation of murine adipose tissues (Fig. 1I).

Identical to the FACS-sorted primary murine white preadipocytes, cultured primary human subcutaneous preadipocytes had very low levels of *Asc-1*, but expression was induced upon differentiation to mature adipocytes *in vitro* (Fig. 1J). *Asc-1* expression in human adipocytes was similar to the expression pattern of *leptin*, a classical white adipocyte marker (Fig. 1J).

Identification of brown adipocyte cell surface markers

To identify brown adipocyte-specific surface proteins, we performed the same type of database search as shown in fig. S1A, using the brown adipocyte-specific mitochondrial protein uncoupling protein-1 (*UCP-1*) as a reference gene (fig. S1C). We identified two potential brown fat specific transmembrane proteins: G protein-coupled receptor 119

(*Gpr119*) and proton assistant amino acid transporter-2 (*PAT2*). As shown in figs. S5 and S6, on further analysis *Gpr119* was widely expressed, and its expression was similar in adipocytes and the SVF.

By contrast, *PAT2* expression was mostly restricted to mouse adipose tissue, with 3.5- to 7.5-fold greater expression in BAT than WAT depots, and very low levels (1–7% of the levels in BAT) in heart, lung, gallbladder, pancreas and adrenal gland (Fig. 2A). Upon cell fractionation, *PAT2* expression was restricted to adipocytes, with minimal expression in the SVF, and was significantly more highly expressed in brown than white adipocytes (Fig. 2B). Likewise, *PAT2* expression was very low in immortalized murine brown preadipocytes, but its expression was highly induced upon differentiation (Fig. 2C). Interestingly, *PAT2* expression was also observed in white adipocytes differentiated from immortalized subcutaneous mouse SVF (fig. S4), indicating again that these brown and white adipocyte markers were no longer specific in these immortalized cells.

As with *Asc-1*, we did not observe differences in the very low levels of *PAT2* expression in white fat of obese *db*/*db* mice compared with *db*/+ mice (Fig. 2D). However, there was a moderate but significant downregulation of *PAT2* in *db/db* mice compared to *db*/+ mice (Fig. 2D). This observation supports a decrease in brown adipocytes at the expense of white adipocytes.

Western blots of subcutaneous and perigonadal white fat and interscapular brown fat from C57Bl/6 mice showed detectable levels of PAT2 only in BAT (Fig. 2E). Immunostaining of PAT2 in brown adipocytes confirmed the surface localization of PAT2 (Fig. 2F), and this was further validated by membrane fractionation of adipose tissues (Fig. 2G).

We performed another database query with *PAT2* as a reference gene and identified four additional transmembrane proteins on mouse brown adipocytes: *CD300LG*, tetraspanin 18 (*Tspan18*), frizzled-4 (*Fzd4*) and purinergic receptor P2X, ligand-gated ion channel 5 (*P2RX5*). On further analysis *CD300LG*, *Tspan18* and *Fzd4* expression was similar between brown and white adipocytes, as well as the SVF, and showed a broad tissue distribution (figs. S5 and S6). By contrast, *P2RX5* expression was highest in mouse BAT, with very little expression in white adipose tissue. There was also moderate expression in skeletal muscle, heart, brain, adrenal gland, testes, lung, and skin in mice (Fig. 3A) consistent with previous reports (22,23). *P2RX5* was expressed at a higher level in brown adipocytes than in mesenteric or perigonadal white adipocytes or the corresponding SVFs (Fig. 3B). Furthermore, *P2RX5* expression was strongly induced upon differentiation of immortalized murine brown preadipocytes (Fig. 3C).

Unlike *Asc-1* and *PAT2*, which lost their specificity after cell immortalization, *P2RX5* expression remained significantly higher in cultured immortalized brown adipocytes compared to immortalized white adipocytes (fig. S4). *P2RX5* expression in BAT from obese *db/db* mice was decreased compared to the lean *db*/+ controls, yet both genotypes were much more highly expressed in BAT than WAT (Fig. 3D). Consistent with this, P2RX5 protein was found in brown, but not white, fat by Western blotting (Fig. 3E). Likewise P2RX5 was localized to the cell surface, as shown by immunofluorescent staining (Fig. 3F)

and membrane fractionation (Fig. 3G). Staining of P2RX5 showed additional perinuclear staining, suggesting localization also in the endoplasmic reticulum.

Regulation of *Asc-1*, *PAT2* and *P2RX5* during chronic cold exposure and β3 adrenergic stimulation in mice

As demonstrated above, Asc-1 is a white adipocyte-specific surface protein with very little expression in brown adipocytes, whereas PAT2 and P2RX5 are preferentially expressed in brown adipocytes. To study the changes in expression of these markers and their correlations with *UCP-1* and *leptin* during browning of white adipose tissue, i.e. formation of beige fat, we exposed 8-week-old male mice to chronic cold for two weeks and compared them to mice housed at room temperature (Fig. 4A). *Leptin* expression decreased in perigonadal and subcutaneous white fat upon chronic cold exposure and was very low in BAT. *Leptin* was not detectable in hypothalamus and skeletal muscle (tibialis anterior). *Asc-1* mirrored this expression pattern with decreased expression in white fat upon chronic cold exposure. *Asc-1* expression in the hypothalamus was very low, comparable to its expression in brown fat and unaffected by chronic cold exposure (Fig. 4A).

UCP-1 expression increased in mouse brown fat and subcutaneous white fat upon cold exposure compared to fat from mice housed at room temperature (Fig. 4A). Low levels of *UCP-1* were detected in perigonadal fat but not detected in hypothalamus and skeletal muscle (tibialis anterior). Similar to *UCP-1*, *P2RX5* expression increased significantly in brown fat and subcutaneous white fat upon chronic cold exposure, with low expression in skeletal muscle and perigonadal fat. *PAT2* expression was unaltered upon chronic cold exposure in brown fat and subcutaneous fat, which mimicked the expression pattern of the beige fat marker *Prdm16* (Fig. 4A). Hence, while both PAT2 and P2RX5 are markers of brown and beige adipocytes, PAT2 appears to have more similarities to markers of beige fat as opposed to classical brown fat.

To confirm these observations in an independent model of brown adipocyte induction, we treated 4-month-old male mice with daily injections of saline or the β3-adrenergic receptor agonist CL316243 (1 mg/kg) for two weeks, inducing the differentiation of beige adipocytes in WAT depots. As shown above, *Asc-1* expression was significantly higher in perigonadal WAT than subcutaneous WAT ($p= 0.0003$; unpaired two-tailed t-test), and almost undetectable in BAT, with no significant changes upon CL316243 treatment (Fig. 4B). This expression pattern mirrored *leptin* expression (Fig. 4B), although *leptin* mRNA levels increased significantly in BAT with CL treatment. A similar expression pattern was observed for the mouse white adipocyte markers *Hoxc8* and *Hoxc9* (fig. S7A) (24).

UCP-1, a marker of brown fat, was highly expressed in BAT of saline-treated mice, and further increased upon treatment with CL316243. The levels of *UCP-1* expression were also markedly increased in perigonadal (~6000 fold) and subcutaneous fat (~100 fold) upon β3 stimulation, indicating formation of beige/brown adipocytes within these white depots (Fig. 4B). This was confirmed by the presence of UCP-1 positive adipocytes with multilocular lipid droplets in both WAT depots of CL316243-treated mice (Fig. 4C). The BAT cell surface markers *PAT2* and *P2RX5* were also increased (3- to 8-fold) in subcutaneous and perigonadal fat upon chronic treatment with CL316243. In contrast, the expression of the

recently described beige adipocyte markers *Tbx1* and *Tmem26* and the brown adipocyte marker *Prdm16* (7) were not significantly changed upon chronic cold exposure or CL316243 treatment (Fig. 4, A and B; fig. S7). Thus, *PAT2* expression was similar to *Prdm16* in cold-exposed mice, but more similar to *UCP-1* and *P2RX5* in CL316243-treated mice, suggesting pathways in addition to adrenergic signaling contributing to the response to cold exposure.

Asc-1, *PAT2* and *P2RX5* in human brown and white fat

To study the expression of *Asc-1*, *PAT2* and *P2RX5* in human adipose tissue, biopsies from three cohorts of patients were studied. In the first cohort we obtained biopsies from subcutaneous, carotid sheath and longus colli fat depots from five different patients undergoing neck surgery. Previously reported histological analysis and gene expression studies on these samples indicated that markers of BAT were highest in the deeper fat (the longus colli depot) and lowest in the superficial depot, whereas markers of white fat showed the opposite pattern (15). In agreement with this, we found that *UCP-1* was more highly expressed in human longus colli fat, followed by carotid sheath fat and almost undetectable in subcutaneous fat (Fig. 5A). This was paralleled by expression of *P2RX5* and *PAT2*, which were high in both of the deeper fat depots and very low in subcutaneous fat (Fig. 5A). Conversely, *leptin* expression was highest in subcutaneous fat biopsies and reduced in the deeper depots. Similar expression was observed for *Asc-1* in all three regions, indicating that human BAT is a mixture of brown and white adipocytes.

To further explore the relationship of *Asc-1*, *PAT2* and *P2RX5*, we performed a comparison to 12 other known markers of different adipose cell lineages. For this comparison we used a total of 24 biopsies from 10 different patients from both superficial (subcutaneous; n=10) and deep (around the carotid sheath, longus colli or prevertebral areas; n=14) fat depots, as previously described (15). For this analysis, each individual deep, brown-enriched fat biopsy was matched with the corresponding superficial (mainly white) fat from the same patient, resulting in 14 paired comparisons. Hierarchical cluster analysis of the deep-to-superficial ratio of expression for each gene identified two major clusters (Fig. 5B). The first cluster of genes exhibited low expression in deep versus superficial fat depots, indicative of white adipocytes. This cluster included *leptin*, *EBF3*, *FBXO31*, *EVA1*, *CD137*, *Tmem26*, *Shox2*, *Hoxc9* and *Asc-1*. The second cluster, reflecting the associations with brown fat observed previously (15), including *UCP-1*, *TBX1*, *Zic1* and *Lhx8* as well as *P2RX5* and *PAT2*.

Finally, to gain further insights into the regulation of these surface markers in human white adipose tissue, we compared expression of *Asc-1*, *PAT2* and *P2RX5* from a third cohort of subjects. These biopsies were obtained from subcutaneous abdominal and intra-abdominal omental fat of lean and obese subjects as previously described (25). Similar to the murine expression pattern, *P2RX5* and *PAT2* were barely detectable or very low in whole tissue or isolated adipocytes from either of these white adipose depots (Fig. 5, C and D). In contrast, *Asc-1* was robustly expressed in all white adipose tissue samples, with significantly higher levels in omental fat compared to subcutaneous fat of obese subjects. Likewise, isolated primary adipocytes from omental fat of obese subjects showed a two-fold higher expression of *Asc-1* than subcutaneous adipocytes, with very low levels of expression in the

corresponding SVF (Fig. 5D). In lean subjects, there was no significant difference between subcutaneous and omental fat expression of *Asc-1* (Fig. 5C).

Discussion

Adipose tissue plays a critical role in whole body energy homeostasis. White adipose tissue stores energy in the form of triglycerides, whereas brown and beige adipose tissues utilize energy through mitochondrial uncoupling. The adipocytes that compose these tissues also differ in their developmental origin and gene expression profile (26). Thus, white adipocytes have high levels of expression of *leptin* and *adiponectin*, whereas brown adipocytes express high levels of *UCP-1*, *Zic1*, and *Lhx8*, and beige adipocytes express *Tbx1*, *Tmem26* and *Tnsfrsf9*, in addition to *UCP-1*, although the specificity of some of these markers is still debated (27). The ability to use these markers to separate individual cell types *in vitro* or *in vivo* is limited for several reasons. Most of these “markers” are either secreted or intracellular proteins, and many are not exclusive to one adipocyte subtype. Some even show high levels of expression in non-adipose tissues. Furthermore, adipose depots can be heterogeneous containing different types of adipocytes, which can change over time or upon physiological, pathophysiological or pharmacological stimulation. Hence, to fully understand the nature and function of adipose depots and to therapeutically exploit the beneficial effects of increasing brown and/or beige adipose tissue mass and function, it is essential to find appropriate markers to distinguish these cell types *in vivo*.

The goal of this study was to identify novel white and brown adipocyte-specific cell surface markers that could be used to mark and target these cells *in vitro* and *in vivo*. Using a gene expression database, we were able to identify several surface proteins that are coordinately expressed with *adiponectin* (a marker of white adipocytes) or with *UCP-1* (a marker of brown/beige adipocytes). While a number of these genes had a broader pattern of expression than initially anticipated or had higher expression in the SVF than in the adipocytes themselves, three markers had the characteristics that were sought: *Asc-1*, *PAT2* and *P2RX5*.

Asc-1 is highly enriched in white adipocytes, with very low expression in the SVF and most other peripheral tissues. *Asc-1* expression is also very low in white preadipocytes, but strongly induced upon differentiation, indicating that *Asc-1* is a marker of mature adipocytes. Among white adipose tissues, *Asc-1* expression is higher in visceral adipose tissue depots than in subcutaneous fat in both mice and humans. These differences are also observed in freshly isolated human subcutaneous and omental adipocytes, and thus appear to reflect intrinsic differences in adipose tissue depots. Interestingly, *Asc-1* expression was upregulated in subcutaneous fat of obese leptin-deficient *ob/ob* mice, but not in the same depot in leptin receptor-deficient *db/db* mice or HFD fed mice. It will be important to determine the regulatory elements modulating *Asc-1* expression in general and specifically during obesity.

Previous expression analysis in mice and humans revealed predominant expression of *Asc-1* in brain, with low levels of expression in lung, small intestine, placenta, kidney and heart. Thus most physiological studies of *Asc-1* have focused on brain. However, the tissue panels used for these earlier Northern blot experiments did not include either white or brown

adipose tissue (19,20). Our expression analysis of *Asc-1* also revealed significant expression in various brain regions, but *Asc-1* expression in white fat is at least 5-fold higher than in any region of the brain tested.

Asc-1, also known as solute carrier family 7 member 10, is encoded by the SLC7A10 gene and is a plasma membrane localized sodium-independent, neutral amino acid exchange transporter. In brain, Asc-1 has high affinity for D-serine, an activator of glutamate/N-methyl-D-aspartate (NMDA) receptors (19,20,28). Mice deficient for Asc-1 show tremors, seizures and reduced body weight leading to lethality within 30 days after birth (29). While the function of Asc-1 in adipose tissue needs further study, in contrast to leptin and adiponectin, which are the most commonly used markers of white adipose tissue, Asc-1 is not a secreted hormone, but a protein that marks the surface of white adipocytes. In addition, Asc-1 shows a greater specificity for white adipose tissue compared to brown adipose tissue than both leptin and adiponectin. Thus, agents like antibodies, aptamers and other molecules could be designed to target Asc-1, providing a unique approach for identification and delivering drugs to white adipocytes. Interestingly, the specificity of Asc-1 for white over brown adipocytes seen *in vivo* and in primary cultures of SVF is lost in immortalized brown adipocytes, suggesting that immortalization causes a loss of the repression of this white adipose marker observed *in vivo*. These data highlight the necessity of screens with primary adipocytes or *in vivo* screens to identify cell type specific markers since significant changes in expression can occur *in vitro* and/or after immortalization.

In addition to Asc-1 as a marker of white adipocytes, we identified two cell surface markers of brown/beige adipocytes, PAT2 and P2RX5. PAT2 is part of a four-member family of proton coupled amino acid transporters, with high affinity for proline, glycine, alanine and hydroxyproline (30,31). PAT2 shows the highest specificity for adipose tissue among all three markers identified in this study and can be detected in both white and brown adipocytes, although with significantly higher expression in brown fat. In humans, mutations in *PAT2* are associated with an iminoglycinuric phenotype (32), although we and others (33) could detect no significant expression of *PAT2* in kidney. Brown preadipocytes express very low levels of *PAT2*, but expression is highly induced upon differentiation, similar to the behavior of *Asc-1* in white preadipocytes. The differences in *PAT2* expression between fat depots are smaller in isolated white and brown adipocytes compared to whole tissues, despite very low expression in the SVF. This discrepancy could result from contamination of white adipocytes in the brown adipocyte isolations, which show a lower density and preferentially float during the isolation.

P2RX5 is part of a seven-member family of ATP gated ion channels (30,31), with highest expression in brown adipocytes and brown adipose tissue. Unlike *PAT2*, however, expression of *P2RX5* is very low in white fat, making it more brown fat specific, although moderate expression can be detected in skeletal muscle and heart. In contrast to the other two cell surface markers, *P2RX5* is also expressed in brown preadipocytes, and its expression is further increased upon differentiation. However, as with *Asc-1*, both *PAT2* and *P2RX5* are also expressed in differentiated adipocytes from immortalized cultured white and brown fat derived from SVF, although expression of *P2RX5* remains significantly higher in brown versus white adipocytes. These data show that while certain characteristics of white

and brown adipocytes, such as *UCP-1* expression, persist upon prolonged culture, whereas other differences can be lost under these conditions. Thus great care needs to be taken in the interpretation of white versus brown or beige markers without *in vivo* validation.

Although both PAT2 and P2RX5 are brown fat specific, they differ in their response to cold exposure and β3 adrenergic stimulation with CL316243. *P2RX5* expression increases in BAT and subcutaneous white fat following both stimuli and also increased in perigonadal white fat upon CL316243 treatment. This mimics the response of *UCP-1* expression in these same fat depots. In contrast, *PAT2* does not change its expression in any fat depot upon chronic cold exposure, but is strongly increased in subcutaneous and perigonadal white fat to levels equal to that of BAT in CL316243 treated mice. Thus, it is tempting to speculate that PAT2 and P2RX5 mark distinct brown/beige adipocyte populations. This is in line with recent studies suggesting that mixtures of beige and brown adipocytes may co-exist within white adipose depots (7,15,16).

Several genes have been described as being useful to differentiate between constitutive brown and inducible beige adipocytes. However, most of these gene products, including Tbx1, Hoxc8, Hoxc9, Zic1 and Lhx8 are nuclear proteins, and therefore not easily accessible for targeting *in vivo*. In contrast, PAT2 and P2RX5, as well as the previously described Tmem26 and Tnfrsf9, are cell surface proteins. These latter genes were identified by comparison of white and brown adipose tissue or selecting single cell preadipocyte clones from white fat pads. Hence, by the nature of the experimental design, which focused on a comparison of brown or beige adipocytes, there was limited analysis of non-adipose tissues (27). As a result these markers provide interesting tools to study the development of different adipose tissue depots and cell types, but do not provide useful markers to target brown fat *in vivo*. In contrast, PAT2 and P2RX5 fulfill all requirements to be used for targeting for drug delivery to brown/beige fat *in vivo* as they are localized on the cell surface and show a very high specificity for brown adipocytes compared to more than 40 other tissues.

Analysis of human neck fat biopsies confirms the expression of *P2RX5* and *PAT2* in human brown adipose tissue. *P2RX5* and *PAT2* are highly expressed in deep cervical fat, i.e. fat near the carotid sheath or longus colli muscle, fat depots which are known to contain cells with high *UCP-1* expression (15). In the current study samples, we find that *UCP-1* expression is higher in longus colli fat than carotid sheath fat. Since the expression of *UCP-1* reflects the amount of brown fat, as well as its state of activity (34), the relatively lower levels of *UCP-1* with high levels of *P2RX5* and *PAT2* in the carotid sheath fat may indicate the presence of inactive or less active brown fat in these areas. To date, identification and classification of brown fat in humans relies mainly on PET scanning techniques using ^{18}F-fluorodeoxyglucose uptake into metabolically active brown adipocytes. Although there are some reports indicating that MRI can also assess brown fat in humans (35), most current imaging methods do not allow quantification of inactive brown fat, which would be essential if one is to determine total response of brown fat mass to any physiological alterations or pharmacological stimulation. Thus, future experiments directed at finding appropriate antibodies or other targeting molecules to extracellular epitopes of

Asc-1, PAT2 and P2RX5 should allow both quantitative imaging and targeting of drugs *in vivo* to brown and white fat.

In conclusion, the cell surface proteins Asc-1, PAT2 and P2RX5 provide novel tools to selectively mark and access intact white and brown adipocytes *in vivo* and in primary isolated cells *in vitro*. These markers, and agents directed against them, could be used to dissect the heterogeneity and intrinsic differences of adipose tissue depots, as well as for diagnostic and therapeutic purposes.

Materials and Methods

Study design

The overall objective of this study was to identify novel white and brown adipocytes cell surface markers in mice and validate their specificity in human fat tissue biopsies. To identify potential candidate genes, we performed a query using the murine biopgps database (www.biogps.org) to identify surface proteins with a correlated gene expression pattern to the white adipocyte marker *adiponectin* and the brown adipocyte marker *UCP-1*. Candidate genes were tested by qPCR on multiple tissues of wild type C57Bl/6 mice and their expression pattern was studied in genetically obese *ob/ob* and *db/db* mice, as well as mice made obese by feeding a high fat diet and mice stimulated to activate brown fat and induce browning of white adipose tissue, namely chronic cold exposure and treatment with the β3-adrenergic receptor agonist CL316243. White and brown adipocyte specificity and membrane localization were validated by Western blot and immunofluorescence staining of selected candidate genes. These observations in mice were translated to humans by using white and brown fat biopsies from three previously published (15,25) patient cohorts.

Mice

All protocols were approved by the Institutional Animal Care and Use Committee of the Joslin Diabetes Center and in accordance with NIH guidelines. Mice (Jackson Lab) were maintained on a 12 h-light/dark cycle and fed a normal chow diet (9F5020; PharmaServ). To induce browning of white fat, 8-week-old C57Bl/6 male mice were housed at 5°C in a thermo-controlled incubator under the same diet and light conditions for two weeks. In addition 4-month-old male mice on a mixed C57Bl/6 and 129Sv background were injected intraperitoneally with either saline or CL316243 (1 μg/g body weight) daily for 14 days, as described previously (3). To study the effects of high fat diet (HFD; D12492) induced expression changes, 4-month-old male mice on a mixed C57Bl/6 and 129Sv background were fed a HFD diet containing 60% calories from fat for 8 weeks. For tissue expression studies, 7-week-old C57Bl/6 mice were anesthetized and perfused with PBS using intracardiac perfusion prior to tissue harvest. Tissues from 12 week-old-male C57Bl/6 *db*/*db* and *db*/+ as well as *ob/ob* and *ob*/+ mice were also collected, but without intracardiac perfusion.

Human study population

Human brown fat and corresponding superficial white fat biopsies were obtained during anterior cervical spine surgery or thyroidectomy (n = 24 biopsies from 10 patients). Written

informed consent was obtained before surgery (15). All patients undergoing thyroidectomies had thyroid-stimulating hormone values within the normal range. This study followed the institutional guidelines of and was approved by the Human Studies Institutional Review Boards of Beth Israel Deaconess Medical Center and Joslin Diabetes Center.

In additional cohorts, human fat biopsies were obtained from the abdominal region of lean and obese subjects, with written informed consent. The study was approved by the regional committee for Medical and Health Research Ethics, Western Norway (REK Vest). Expression was compared between whole subcutaneous and omental fat from lean and obese subjects, and between isolated subcutaneous and omental adipocytes and SVF from obese subjects. An overview of the cohorts is shown in table S1. In some studies whole tissue was collected by surgical excision during bariatric surgery (obese subjects) or elective surgery (lean subjects), and immediately placed in liquid nitrogen. Adipocytes and SVF were separated as described previously (25). Briefly, about 700–800 mg of tissue was fractionated by collagenase for 30 minutes at 37°C immediately after excision. The released cells were sieved through a 200 μm polypropylene filter. Floating cells (adipocytes) were transferred to a 2 ml tube, washed in 1 ml Hanks' Balanced Salt Solution (HBSS) with 5% bovine serum albumin (BSA), and collected after floating. The non-floating cells (SVF) were centrifuged at 2,500 rpm for 5 min, and the supernatant was removed. The adipocytes and SVF were lyzed in Qiazol Lysing Reagent (Qiagen) and frozen in liquid nitrogen.

Adipocyte marker identification

The expression pattern of mouse *adiponectin* and *UCP-1* were used to search the Symatlas database (www.biogps.org) for genes with correlated (coefficient greater than 0.95) expression pattern. These candidate genes were filtered for high expression in fat (at least 3 times the mean of all other tissues) with less than the mean levels of expression in skeletal muscle, heart, lung, pancreas cerebellum and cerebral cortex. Identified candidates were used for further validation.

Real Time PCR

Murine tissues and human neck fat biopsies were collected, and total RNA was extracted using the Qiagen RNeasy Mini kit. Total RNA (1 μg) was reverse transcribed with random hexamer primers (Applied Biosystems) in 20 μl and subsequently diluted 1:10 with water. qPCR was performed using SYBR green (BioRad), 300 nM of primers and 2.5 μl of cDNA per well in a final volume of 10 μl. Each sample was tested either in duplicate or triplicate.

For human subcutaneous and omental fat, RNA was isolated by the RNeasy Lipid Tissue Midi Kit (Qiagen). cDNA was synthesized from 0.5–1 μg RNA per sample using the Transcriptor First Strand cDNA Synthesis Kit (Roche) or the SuperScript VILO cDNA Synthesis Kit (Invitrogen), and was diluted 1:20 before qPCR. qPCR was performed with SYBR Green PCR mix (Biorad) using the LightCycler480 system (Roche) with 15 min initial activation at 95°C, 40 cycles of 15 sec at 95°C, 30 sec at 60°C, and 30 sec at 72°C. Specific amplification of transcripts was confirmed by melting curve analysis at the end of each PCR. Mean target mRNA levels based on technical triplicates were calculated by the ΔΔCT method, normalized to the level of TATA-binding protein (*TBP*) measured by the

Universal ProbeLibrary Human TBP Gene Assay (Roche). The primers for mouse and human qPCR used are in table S2.

Mouse adipocyte and preadipocyte isolation and flow cytometry

Adipocytes from perigonadal, flank, inguinal, and subcutaneous white fat, and brown adipose depots from each individual mouse were isolated by collagenase digestion (36). Briefly, mouse adipose tissues were minced and incubated in DMEM containing 1% BSA and 1 mg/ml collagenase type I (Worthington, CLS-1) for 30–40 minutes at 37°C und constant shaking. Undigested material was removed by straining through a 200–250 micron nylon mesh. Cells were washed with PBS. Adipocytes were collected by pipetting off the floating cells, and cells of the stromal vascular fraction were collected by centrifugation. Isolation of adipocyte precursors was performed using SVF from perigonadal and subcutaneous mouse fat pads and preadipocytes were sorted by an Aria flow cytometer (BD Biosciences). Preadipocytes were defined as being negative for Ter119, CD45, and CD31 and positive for both SCA1 and CD34 (21).

Adipocyte differentiation

Primary human subcutaneous preadipocytes and media were purchased (Lonza Inc.), grown and differentiated following the manufacturer's instructions. Briefly, cells were grown in preadipocyte growth media, plated into 12-well plates, and grown until confluent. Fresh adipocyte differentiation medium was added every two days until day 10. Murine primary white preadipocytes were cultured and differentiated as described previously (21). Brown adipocyte differentiation was induced in confluent brown preadipocytes (1 day after reaching confluence) with 100 nM insulin, 1 nM triiodothyronine, 0.5 mM isobutylmethylxanthine, 1 μM dexamethasone, and 0.125 mM indomethacin in DMEM high glucose with 10% FBS for 48 h. Following, cells were kept in medium containing 10% FBS, 100 nM insulin, and 1 nM triiodothyronine.

For immunofluorescent staining, we used immortalized cells obtained from the SVF of subcutaneous white and interscapular brown fat of Immorto mice [CBA; B10-Tg(H2Kb-tsA58)6Kio/Crl] from Charles River. These cells were grown at 33°C where they expressed a temperature-sensitive SV40 TsA58 mutant that becomes inactivated at 37 °C. For differentiation, cells were plated on chamber slides, grown until they reached confluence and differentiated at 37 °C in DMEM high glucose containing 20% FBS, 20 μM insulin, 1 nM T3, 0.5 mM IBMX, 1 μM rosiglitazone, and 125 μM indomethacin for two days and further differentiated in DMEM 20% FBS, 20 μM insulin, 1 nM T3, and 1 μM rosiglitazone for two days, and then in 20% FBS, 20 μM insulin, and 1 nM T3 for two more days.

Membrane fractionation and Western blot

Subcutaneous, perigonadal and brown adipose tissues from 8 week-old C57Bl/6 mice were homogenized in RIPA buffer containing protease inhibitors (P8340; Sigma) using a TissueLyser II (Qiagen). Equal amounts of protein were loaded on 8% acrylamide gels, and membranes were blotted for Asc-1 (Abnova 1:500), PAT2 (Santa Cruz, 1:500), and P2RX5 (Abcam, 1:10.000). For membrane isolations, fat depots were homogenized in 250 mM sucrose, 1 mM EDTA, 10 mM Tris (pH 7.4) containing protease inhibitors with 10 strokes

of a Dounce homogenizer. Post-nuclear supernatants were centrifuged for 20 min at 16,000 g. Membrane pellets were resuspended in RIPA buffer containing protease inhibitors. The cytoplasm was centrifuged for 45 min at 160,000 g to remove microsomes. Equal volumes were loaded for Western blotting as described above.

Immunofluorescent staining of mouse adipocytes

Twelve hours prior to staining, cells were treated with D-3860 4,4-difluoro-5-(4-phenyl-1,3-butadienyl)-4-bora-3a,4a-diaza-s-indacene-3-pentanoic acid (BODIPY 581/591 C5; 1:10,000). Cells were fixed with PFA, permeabilized using 0.5% Triton-X, blocked with 3% BSA and 10% normal goat serum in 0.1% Tween-20/ PBS, and incubated for 2 hours with primary antibody: Asc1 (Abnova PA8453; 1:50), PAT2 (Santa Cruz sc390969; 1:100), or P2XR5 (Abcam ab82327; 1:1000). An Alexa-Fluor-488 goat anti-rabbit IgG, or Alexa-Fluor-488 goat-anti mouse IgG (Invitrogen; 1:500) was used as a secondary antibody, and slides were mounted with Vectashield containing DAPI. Image acquisition was performed using a Zeiss 710 confocal microscope.

Statistical Analysis

Data are presented as means ± SEM. All statistical analysis was performed using GraphPad Prism. Normal distribution of samples was tested, where appropriate, to select parametric or non-parametric tests as indicated in the figure legends. Two-tailed Student’s t test or 1-or 2-Way ANOVA for multiple comparisons was used to determine p values, unless indicated differently in the figure legend.

Supplementary Material

Refer to Web version on PubMed Central for supplementary material.

Acknowledgments

We thank J. Fernø and E. Grytten for expert technical assistance.

Funding: This study was supported by National Institutes of Health Grant DK82659. SU was supported by a Human Frontiers Longterm Fellowship. A.K. was supported by a grant from the German Research Foundation (DFG) project Kl2399-1/1.

References and Notes

1. Tchkonia T, Lenburg M, Thomou T, Giorgadze N, Frampton G, Pirtskhalava T, Cartwright A, Cartwright M, Flanagan J, Karagiannides I, Gerry N, Forse RA, Tchoukalova Y, Jensen MD, Pothoulakis C, Kirkland JL. Identification of depot-specific human fat cell progenitors through distinct expression profiles and developmental gene patterns. Am J Physiol Endocrinol Metab. 2007; 292:E298–E307. [PubMed: 16985259]
2. Flier JS. Obesity wars: molecular progress confronts an expanding epidemic. Cell. 2004; 116:337–350. [PubMed: 14744442]
3. Boucher J, Mori MA, Lee KY, Smyth G, Liew CW, Macotela Y, Rourk M, Bluher M, Russell SJ, Kahn CR. Impaired thermogenesis and adipose tissue development in mice with fat-specific disruption of insulin and IGF-1 signalling. Nat Commun. 2012; 3:902. [PubMed: 22692545]
4. Atit R, Sgaier SK, Mohamed OA, Taketo MM, Dufort D, Joyner AL, Niswander L, Conlon RA. Beta-catenin activation is necessary and sufficient to specify the dorsal dermal fate in the mouse. Dev Biol. 2006; 296:164–176. [PubMed: 16730693]

5. Seale P, Bjork B, Yang W, Kajimura S, Chin S, Kuang S, Scime A, Devarakonda S, Conroe HM, Erdjument-Bromage H, Tempst P, Rudnicki MA, Beier DR, Spiegelman BM. PRDM16 controls a brown fat/skeletal muscle switch. Nature. 2008; 454:961–967. [PubMed: 18719582]
6. Tseng YH, Cypess AM, Kahn CR. Cellular bioenergetics as a target for obesity therapy. Nat Rev Drug Discov. 2010; 9:465–482. [PubMed: 20514071]
7. Wu J, Bostrom P, Sparks LM, Ye L, Choi JH, Giang AH, Khandekar M, Virtanen KA, Nuutila P, Schaart G, Huang K, Tu H, van Marken Lichtenbelt WD, Hoeks J, Enerback S, Schrauwen P, Spiegelman BM. Beige adipocytes are a distinct type of thermogenic fat cell in mouse and human. Cell. 2012; 150:366–376. [PubMed: 22796012]
8. Liu W, Shan T, Yang X, Liang S, Zhang P, Liu Y, Liu X, Kuang S. A heterogeneous lineage origin underlies the phenotypic and molecular differences of white and beige adipocytes. J Cell Sci. 2013; 126:3527–3532. [PubMed: 23781029]
9. Rosenwald M, Perdikari A, Rulicke T, Wolfrum C. Bi-directional interconversion of brite and white adipocytes. Nat Cell Biol. 2013; 15:659–667. [PubMed: 23624403]
10. Gesta S, Bluher M, Yamamoto Y, Norris AW, Berndt J, Kralisch S, Boucher J, Lewis C, Kahn CR. Evidence for a role of developmental genes in the origin of obesity and body fat distribution. Proc Natl Acad Sci US A. 2006; 103:6676–6681.
11. Stanford KI, Middelbeek RJ, Townsend KL, An D, Nygaard EB, Hitchcox KM, Markan KR, Nakano K, Hirshman MF, Tseng YH, Goodyear LJ. Brown adipose tissue regulates glucose homeostasis and insulin sensitivity. J Clin Invest. 2013; 123:215–223. [PubMed: 23221344]
12. Saito M, Okamatsu-Ogura Y, Matsushita M, Watanabe K, Yoneshiro T, Nio-Kobayashi J, Iwanaga T, Miyagawa M, Kameya T, Nakada K, Kawai Y, Tsujisaki M. High incidence of metabolically active brown adipose tissue in healthy adult humans: effects of cold exposure and adiposity. Diabetes. 2009; 58:1526–1531. [PubMed: 19401428]
13. Cypess AM, Lehman S, Williams G, Tal I, Rodman D, Goldfine AB, Kuo FC, Palmer EL, Tseng YH, Doria A, Kolodny GM, Kahn CR. Identification and importance of brown adipose tissue in adult humans. N Engl J Med. 2009; 360:1509–1517. [PubMed: 19357406]
14. Marken Lichtenbelt WD, Vanhommerig JW, Smulders NM, Drossaerts JM, Kemerink GJ, Bouvy ND, Schrauwen P, Teule GJ. Cold-activated brown adipose tissue in healthy men. N Engl J Med. 2009; 360:1500–1508. [PubMed: 19357405]
15. Cypess AM, White AP, Vernochet C, Schulz TJ, Xue R, Sass CA, Huang TL, Roberts-Toler C, Weiner LS, Sze C, Chacko AT, Deschamps LN, Herder LM, Truchan N, Glasgow AL, Holman AR, Gavrila A, Hasselgren PO, Mori MA, Molla M, Tseng YH. Anatomical localization, gene expression profiling and functional characterization of adult human neck brown fat. Nat Med. 2013
16. Jespersen NZ, Larsen TJ, Peijs L, Daugaard S, Homoe P, Loft A, de Jong J, Mathur N, Cannon B, Nedergaard J, Pedersen BK, Moller K, Scheele C. A classical brown adipose tissue mRNA signature partly overlaps with brite in the supraclavicular region of adult humans. Cell Metab. 2013; 17:798–805. [PubMed: 23663743]
17. Walden TB, Hansen IR, Timmons JA, Cannon B, Nedergaard J. Recruited vs. nonrecruited molecular signatures of brown, “brite,” and white adipose tissues. Am J Physiol Endocrinol Metab. 2012; 302:E19–E31. [PubMed: 21828341]
18. Lee KY, Russell SJ, Ussar S, Boucher J, Vernochet C, Mori MA, Smyth G, Rourk M, Cederquist C, Rosen ED, Kahn BB, Kahn CR. Lessons on conditional gene targeting in mouse adipose tissue. Diabetes. 2013; 62:864–874. [PubMed: 23321074]
19. Fukasawa Y, Segawa H, Kim JY, Chairoungdua A, Kim DK, Matsuo H, Cha SH, Endou H, Kanai Y. Identification and characterization of a Na(+)-independent neutral amino acid transporter that associates with the 4F2 heavy chain and exhibits substrate selectivity for small neutral D- and L-amino acids. J Biol Chem. 2000; 275:9690–9698. [PubMed: 10734121]
20. Nakauchi J, Matsuo H, Kim DK, Goto A, Chairoungdua A, Cha SH, Inatomi J, Shiokawa Y, Yamaguchi K, Saito I, Endou H, Kanai Y. Cloning and characterization of a human brain Na(+)-independent transporter for small neutral amino acids that transports D-serine with high affinity. Neurosci Lett. 2000; 287:231–235. [PubMed: 10863037]

21. Macotela Y, Emanuelli B, Mori MA, Gesta S, Schulz TJ, Tseng YH, Kahn CR. Intrinsic differences in adipocyte precursor cells from different white fat depots. Diabetes. 2012; 61:1691–1699. [PubMed: 22596050]
22. Cox JA, Barmina O, Voigt MM. Gene structure, chromosomal localization, cDNA cloning and expression of the mouse ATP-gated ionotropic receptor P2X5 subunit. Gene. 2001; 270:145–152. [PubMed: 11404011]
23. Le KT, Paquet M, Nouel D, Babinski K, Seguela P. Primary structure and expression of a naturally truncated human P2X ATP receptor subunit from brain and immune system. FEBS Lett. 1997; 418:195–199. [PubMed: 9414125]
24. Yamamoto Y, Gesta S, Lee KY, Tran TT, Saadatirad P, Kahn CR. Adipose depots possess unique developmental gene signatures. Obesity (SilverSpring). 2010; 18:872–878.
25. Veum VL, Dankel SN, Gjerde J, Nielsen HJ, Solsvik MH, Haugen C, Christensen BJ, Hoang T, Fadnes DJ, Busch C, Vage V, Sagen JV, Mellgren G. The nuclear receptors NUR77, NURR1 and NOR1 in obesity and during fat loss. Int J Obes (Lond). 2012; 36:1195–1202. [PubMed: 22143616]
26. Gesta S, Tseng YH, Kahn CR. Developmental origin of fat: tracking obesity to its source. Cell. 2007; 131:242–256. [PubMed: 17956727]
27. Lidell ME, Betz MJ, Enerback S. Two types of brown adipose tissue in humans. Adipocyte. 2014; 3:63–66. [PubMed: 24575372]
28. Rutter AR, Fradley RL, Garrett EM, Chapman KL, Lawrence JM, Rosahl TW, Patel S. Evidence from gene knockout studies implicates Asc-1 as the primary transporter mediating d-serine reuptake in the mouse CNS. Eur J Neurosci. 2007; 25:1757–1766. [PubMed: 17432963]
29. Xie X, Dumas T, Tang L, Brennan T, Reeder T, Thomas W, Klein RD, Flores J, O'Hara BF, Heller HC, Franken P. Lack of the alanine-serine-cysteine transporter 1 causes tremors, seizures, and early postnatal death in mice. Brain Res. 2005; 1052:212–221. [PubMed: 16026768]
30. Garcia-Guzman M, Soto F, Laube B, Stuhmer W. Molecular cloning and functional expression of a novel rat heart P2X purinoceptor. FEBS Lett. 1996; 388:123–127. [PubMed: 8690069]
31. North RA. Molecular physiology of P2X receptors. Physiol Rev. 2002; 82:1013–1067. [PubMed: 12270951]
32. Foltz M, Oechsler C, Boll M, Kottra G, Daniel H. Substrate specificity and transport mode of the proton-dependent amino acid transporter mPAT2. Eur J Biochem. 2004; 271:3340–3347. [PubMed: 15291811]
33. Zebisch K, Brandsch M. Transport of L-proline by the proton-coupled amino acid transporter PAT2 in differentiated 3T3-L1 cells. Amino Acids. 2013; 44:373–381. [PubMed: 22711289]
34. Nedergaard J, Cannon B. UCP1 mRNA does not produce heat. Biochim Biophys Acta. 2013; 1831:943–949. [PubMed: 23353596]
35. Iris Chen YC, Cypess AM, Chen YC, Palmer M, Kolodny G, Kahn CR, Kwong KK. Measurement of Human Brown Adipose Tissue Volume and Activity Using Anatomic MR Imaging and Functional MR Imaging. J Nucl Med. 2013; 54:1584–1587. [PubMed: 23868958]
36. Ussar S, Bezy O, Bluher M, Kahn CR. Glypican-4 Enhances Insulin Signaling Via Interaction With the Insulin Receptor and Serves as a Novel Adipokine. Diabetes. 2012; 61:2289–2298. [PubMed: 22751693]

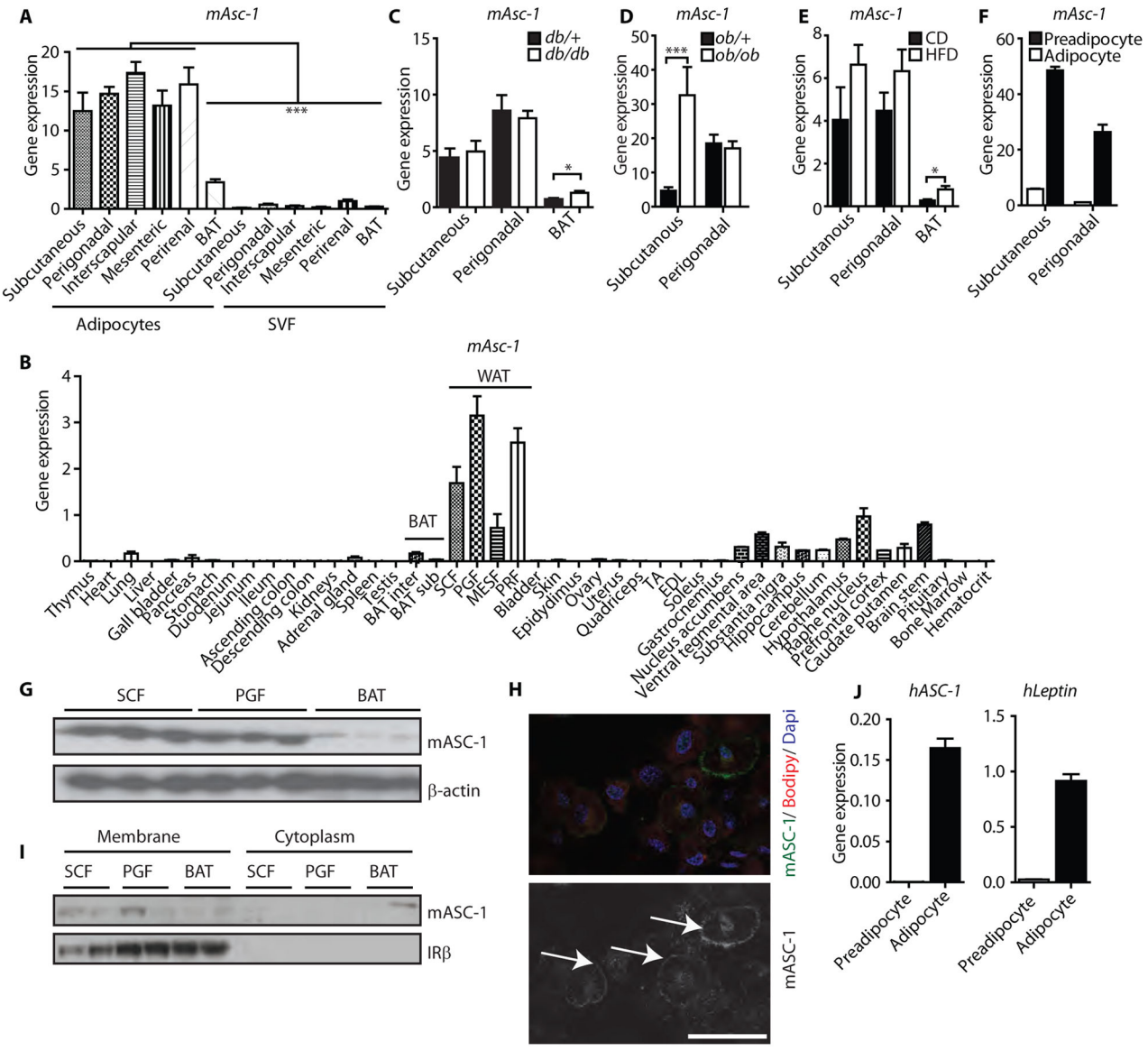

Fig. 1. Asc-1 is a cell surface marker for mouse and human white adipocytes

(**A**) *mAsc-1* expression (qPCR) from freshly isolated mouse adipocytes and their corresponding stromal vascular fraction (SVF) for *mAsc*-1 from different fat depots (n=4 mice). * $p<0.05$, One-Way ANOVA with Tukey's multiple comparison test (**B**) *mAsc-1* expression (qPCR) from 45 tissues from 7 week-old C57BL/6 mice (n=3 mice). Data were normalized to *TBP*. BAT: interscapular brown adipose tissue; SCF: subcutaneous white fat; PGF: perigonadal white fat; MESF: mesenteric white fat; PRF: perirenal white fat. (**C**) *mAsc-1* expression (qPCR) in subcutaneous, perigonadal, and interscapular brown adipose tissues of *db/db* and control (*db*/+) mice, normalized to *TBP* (n=6 mice per group * p<0.05, two-tailed unpaired t-test). (**D**) *mAsc-1* expression (qPCR) in subcutaneous and perigonadal adipose tissues of *ob/ob* and control (ob/+) mice, normalized to *TBP* (n=6 mice per group, ***p< 0.001 –two-tailed unpaired t-test). (**E**) *mAsc-1* expression (qPCR) in subcutaneous, perigonadal, and brown adipose tissues of chow diet (CD) and high fat diet (HFD) fed mice,

normalized to *TBP* (n=4 mice per group, * $p<0.05$, two-tailed unpaired t-test). (**F**) *mAsc-1* expression in primary murine FACS-sorted preadipocytes and mature adipocytes from SCF and PGF (n=2 mice). Data in Panels A to F) are means ± SEM (**G**) Western blot for *mAsc*-1 of SCF, PGF, and BAT. β-actin was used as loading control. The membrane was stripped and reused in figures 2E and 3E, showing the same loading control. (**H**) Immunofluorescent staining of mAsc-1 of differentiated subcutaneous adipocytes from immortalized mouse SVF. Top panel: Cells were co-stained with the lipid dye Bodipy and nuclear dye DAPI. Lower panel: Arrows indicate cell surface staining of Asc-1. Scale bar, 50 μm. (**I**) Western blot of mouse membrane extracts and the corresponding cytoplasmic fractions of SCF, PGF and BAT. IRβ was used as a marker of plasma membrane isolation. (**J**) Expression of human *Asc-1* and *leptin* in primary preadipocytes and fully differentiated (day 10) adipocytes Data are means ± SEM (n=4).

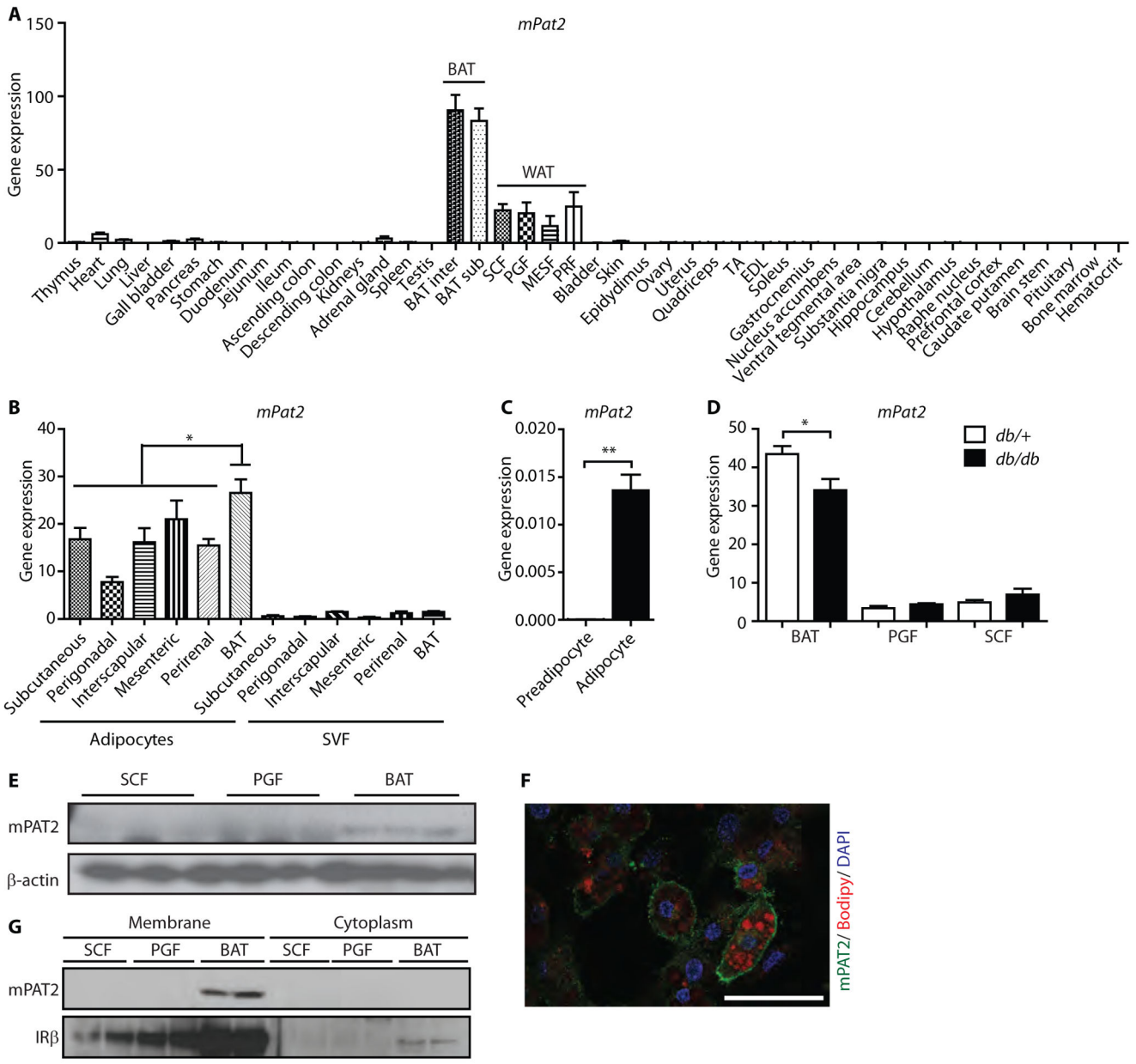

Fig. 2. PAT2 is a cell surface marker of mouse brown adipocytes

(**A**) *mPAT2* expression data from 45 tissues of 7-week old C57BL/6 mice normalized to *TBP*. Data are means ± SEM (n=3 mice). (**B**) *mPat2* expression in freshly isolated adipocytes and their corresponding SVF from different mouse fat depots. Data are means ± SEM (n=4 mice; * p<0.05 One-Way ANOVA with Tukey's multiple comparison test). (**C**) *mPAT2* expression in immortalized murine brown preadipocytes and fully differentiated adipocytes. Data are means ± SEM (n=3 mice; ** p<0.01, two tailed unpaired t-test). (**D**) *PAT2* expression in subcutaneous, perigonadal and brown adipose tissue of *db/db* and control (*db/+*) mice, normalized to *TBP*. Data are means ± SEM (n=6 mice per group; * p<0.05, two tailed unpaired t-test). (**E**) Western blots for mPAT2 of SCF, PGF and BAT. β-actin was used as loading control. The membrane was stripped and reused in figures 1G and

3E, showing the same loading control. (**F**) Immunofluorescent staining of mPAT2 of differentiated brown adipocytes from immortalized SVF, co-stained with the lipid dye Bodipy and nuclear dye DAPI. Scale bar, 50 μm. (**G**) Western blot of membrane extracts and the corresponding cytoplasmic fractions of SCF, PGF and BAT.

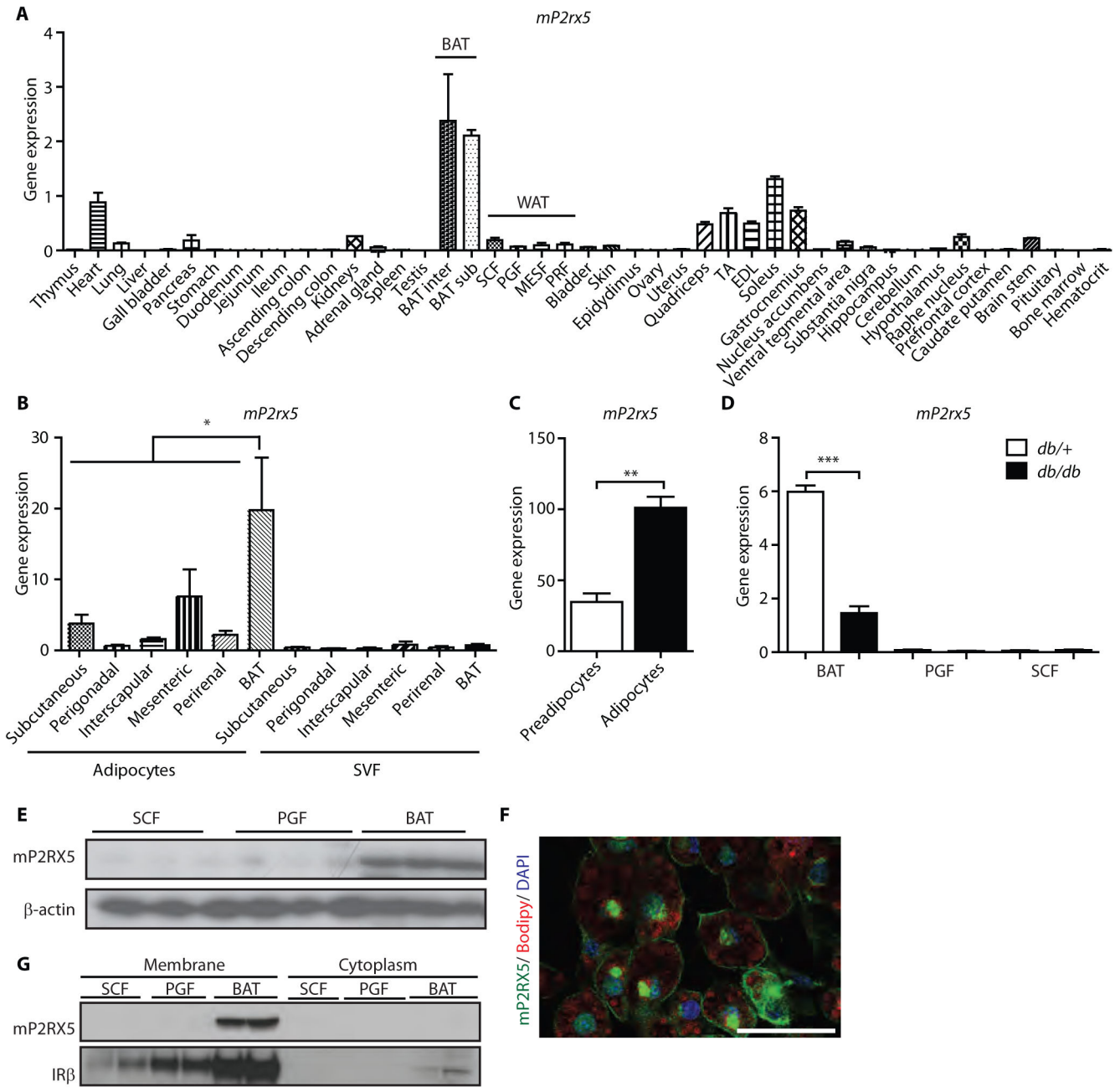

Fig. 3. P2RX5 is a cell surface marker of mouse brown adipocytes

(**A**) *mP2RX5* expression data from 45 tissues of 7-week old C57BL/6 mice normalized to *TBP*. Data are means ± SEM (n=3 mice). (**B**) *mP2RX5* expression in freshly isolated adipocytes and their corresponding SVF from different mouse fat depots. Data are means ± SEM (n=4 mice, * p<0.05 One-Way ANOVA with Tukey's multiple comparison test). (**C**) *mP2RX5* expression in immortalized murine brown preadipocytes and fully differentiated adipocytes. Data are means ± SEM (n=3 mice, ** p<0.01, two tailed unpaired t-test). (**D**) *mP2RX5* expression in subcutaneous, perigonadal and brown adipose tissue of *db/db* and control (*db/+*) mice normalized to *TBP*. Data are means ± SEM (n=6 mice per group; ***

p<0.001, two tailed unpaired t-test). (**E**) Western blots for mP2RX5 of SCF, PGF and BAT. β-actin was used as loading control. The membrane was stripped and reused in figures 1G and 2E, showing the same loading control. (**F**) Immunofluorescent staining of mP2RX5 of differentiated brown adipocytes from immortalized SVF, co-stained with the lipid dye Bodipy and nuclear dye DAPI. Scale bar, 50 μm. (**G**) Western blot of membrane extracts and the corresponding cytoplasmic fractions of SCF, PGF and BAT.

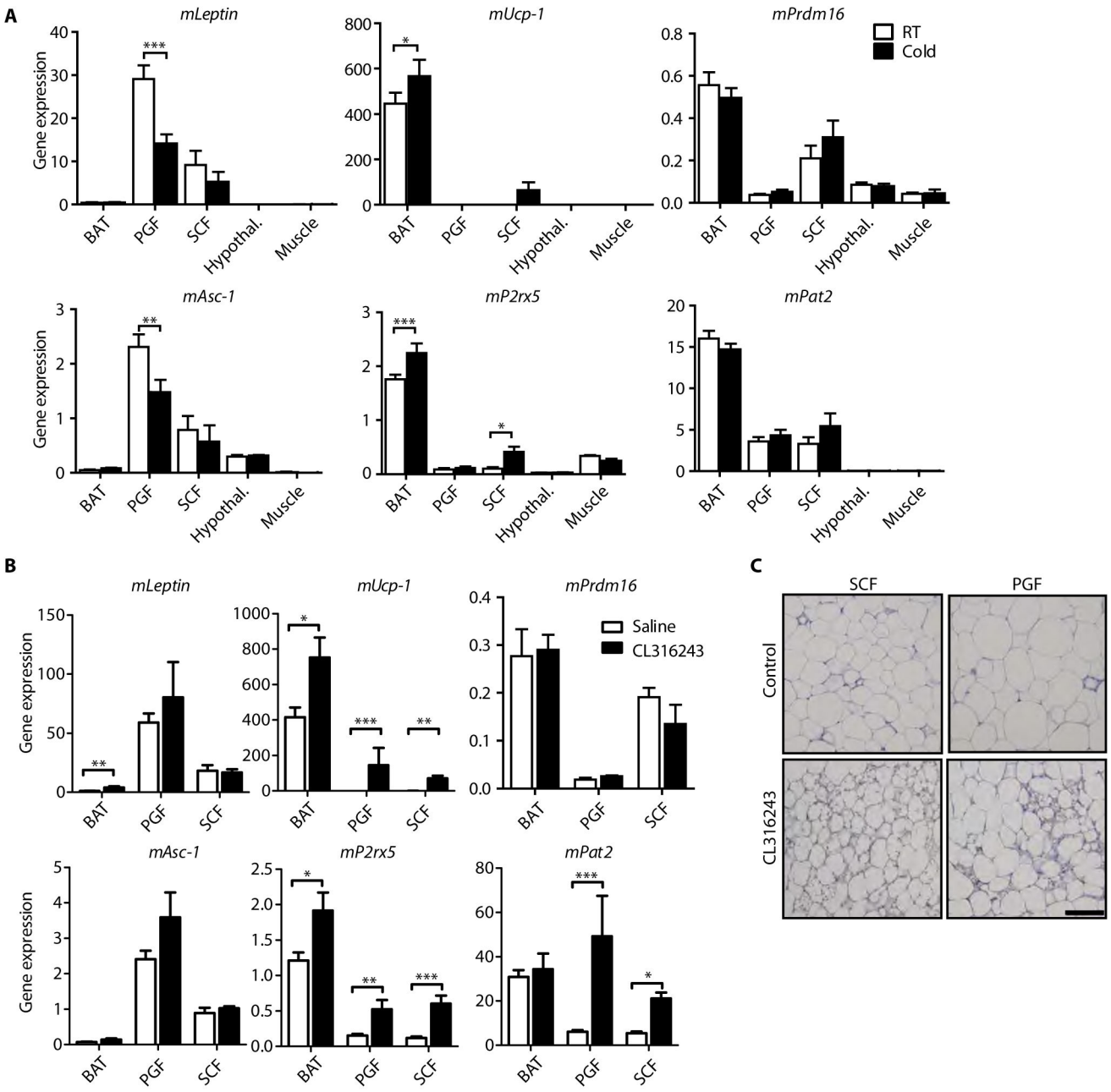

Fig. 4. White and brown adipocyte marker expression upon chronic cold or β3 adrenergic stimulation

(**A**) C57Bl/6 male mice were housed for two weeks at either room temperature or 5°C ("cold"). Gene expression (qPCR) was obtained from BAT, PGF, SCF, hypothalamus, and muscle (tibialis anterior). Data are mean expression normalized to *TBP* ± SEM (n=6 mice per group). (**B**) Gene expression (qPCR) in BAT, PGF, and SCF from saline- or CL316243-treated mice. Data are mean expression normalized to *TBP* ± SEM (n=7 mice per group). In (A and B), **P* < 0.05, ***P*<0.01, ****P*<0.001, Mann-Whitney or two tailed unpaired t-test, where appropriate. **(C)** α-UCP1 immunohistochemistry staining of PGF and SCF from saline- or CL316243-treated mice. Scale bar, 100 μm.

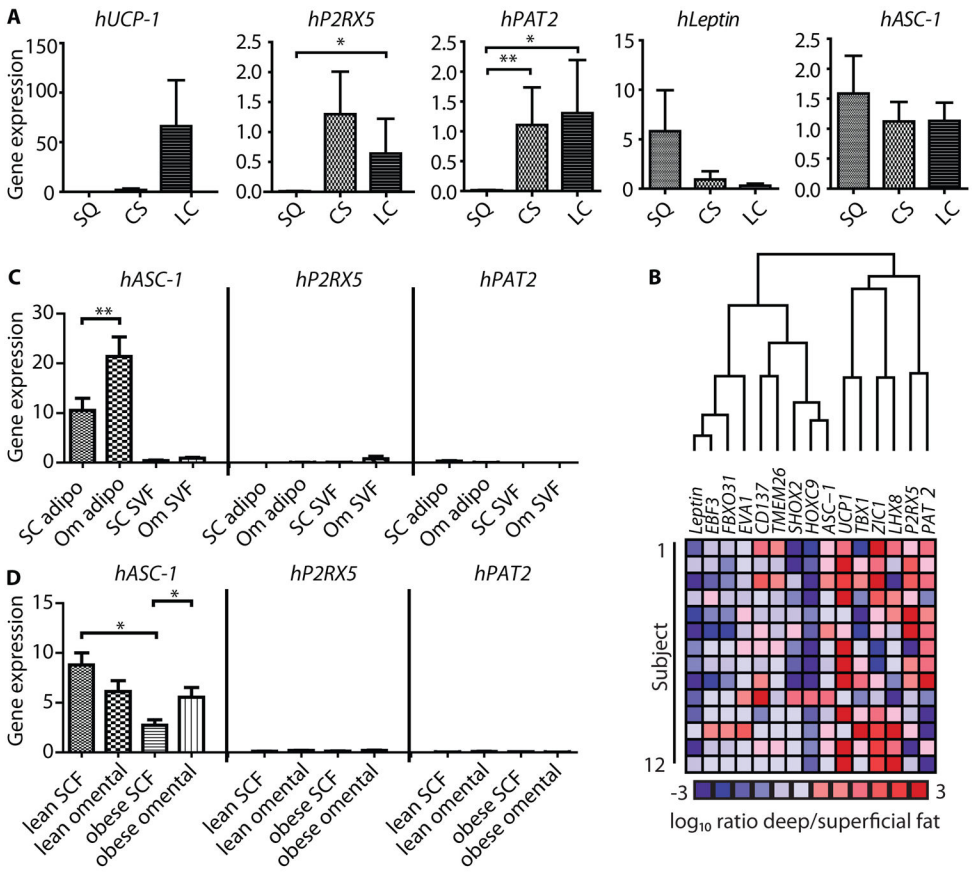

Fig. 5. Expression of Asc-1, PAT2 and P2RX5 in human neck fat biopsies

(A) qPCR normalized to *TBP* of fat biopsies from subcutaneous (SQ), carotid sheath (CS) and the longus colli (LC) areas (n=5) Statistical significance was tested using a Mann Whitney test. **(B)** Cluster analysis of the $\log_{10}$ ratio of gene expression of deep tissues (BAT) to that of superficial (WAT) fat for previously described white, beige and brown adipose tissue markers, as well as *hAsc-1*, *hPAT2* and *hP2RX5* (n=14). **(C)** qPCR for *hAsc-1*, *hPAT2* and *hP2RX5* from isolated subcutaneous (SC) and omental (Om) adipocytes and stromal vascular fraction of obese subjects (n=10). Target mRNA levels were normalized to the level of TBP mRNA, presented as mean ± SEM. (D) qPCR for *hAsc-1*, *hPAT2* and *hP2RX5* of whole subcutaneous (SCF) and omental adipose tissue from obese (n=13 and n=12) and lean (n=37 and n=12) subjects.